Applied Catalysis B: Environmental 193 (2016) 141–150

Contents lists available at ScienceDirect

Applied Catalysis B: Environmental

journal homepage: www.elsevier.com/locate/apcatb

Influence of catalyst synthesis method on selective catalytic reduction (SCR) of NO by NH_3 with V_2O_5-WO_3/TiO_2 catalysts

Yuanyuan He[a,b,1], Michael E. Ford[b], Minghui Zhu[b], Qingcai Liu[a], Uma Tumuluri[c], Zili Wu[c], Israel E. Wachs[b,*]

[a] College of Materials Science and Engineering, Chongqing University, Chongqing 400030, China
[b] Operando Molecular Spectroscopy & Catalysis Laboratory, Department of Chemical Engineering, Lehigh University, Bethlehem, PA 18015, USA
[c] Chemical Science Division and Center for Nanophase Materials Sciences, Oak Ridge National Laboratory, Oak Ridge, TN 37831, USA

ARTICLE INFO

Article history:
Received 17 February 2016
Received in revised form 29 March 2016
Accepted 11 April 2016
Available online 14 April 2016

Keywords:
Catalysts
Supported
TiO_2
V_2O_5
WO_3
Synthesis
Co-precipitation
Incipient-wetness impregnation
Selective catalytic reduction (SCR)
NO
NH_3
O_2
Spectroscopy
Raman
Infrared
TPSR
HS-LEIS
XRD

ABSTRACT

The molecular structures, surface acidity and catalytic activity for NO/NH_3/O_2 SCR of V_2O_5-WO_3/TiO_2 catalysts were compared for two different synthesis methods: co-precipitation of aqueous vanadium and tungsten oxide precursors with $TiO(OH)_2$ and by incipient wetness impregnation of the aqueous precursors on a reference crystalline TiO_2 support (P25; primarily anatase phase). Bulk analysis by XRD showed that co-precipitation results in small and/or poorly ordered TiO_2(anatase) particles and that VO_x and WO_x do not form solid solutions with the bulk titania lattice. Surface analysis of the co-precipitated catalyst by High Sensitivity-Low Energy Ion Scattering (HS-LEIS) confirms that the VO_x and WO_x are surface segregated for the co-precipitated catalysts. *In situ* Raman and IR spectroscopy revealed that the vanadium and tungsten oxide components are present as surface mono-oxo O = VO_3 and O = WO_4 sites on the TiO_2 supports. Co-precipitation was shown *for the first time* to also form new mono-oxo surface VO_4 and WO_4 sites that appear to be anchored at surface defects of the TiO_2 support. IR analysis of chemisorbed ammonia showed the presence of both surface NH_3* on Lewis acid sites and surface NH_4^+* on Brønsted acid sites. TPSR spectroscopy demonstrated that the specific SCR kinetics was controlled by the redox surface VO_4 species and that the surface kinetics was independent of TiO_2 synthesis method or presence of surface WO_5 sites. SCR reaction studies revealed that the surface WO_5 sites possess minimal activity below ~325 °C and their primary function is to increase the adsorption capacity of ammonia. A relationship between the SCR activity and surface acidity was not found. The SCR reaction is controlled by the surface VO_4 sites that initiate the reaction at ~200 °C. The co-precipitated catalysts were always more active than the corresponding impregnated catalysts. The higher activity of the co-precipitated catalysts is ascribed to the presence of the new surface WO_x sites associated surface defects on the TiO_2 support that increase the ammonia adsorption capacity.

1. Introduction

Selective catalytic reduction (SCR) of nitrogen oxides (NO_x) by ammonia is the state-of-the-art NO_x emission control technology for stationary sources, including power plants and industrial boilers [1–3]. Supported VO_x-WO_x/TiO_2 catalysts, which show high SCR activity, thermal stability and resistance to sulfur oxide poisoning, have long been practiced for commercial use [1–7]. As a result, an extensive body of literature exists on both the reactivity and the characterization of supported VO_x-WO_x/TiO_2 catalysts [1–18]. Vanadium oxide provides the active redox component, but due to its undesired activity for oxidation of SO_2 to SO_3, the content of vanadia is usually limited to less than 2% [1,2]. Tungsten oxide acts as a promoter owing to its Brønsted acidity that enhances ammonia adsorption on the catalyst during the SCR reaction [1–8]. The TiO_2(anatase) phase is considered as the best support for SCR catalysts because (i) both vanadium and tungsten oxides can be uniformly dispersed on the surface of TiO_2 below monolayer coverage [2,11,19–21], (ii) the titania support promotes the catalytic activity of the vanadium oxide sites [22], and (iii) TiO_2 is only weakly and reversibly sulfated under SCR reaction conditions in comparison to other supports (*e.g.*, Al_2O_3 and ZrO_2) [2,11,23].

Supported VO_x-WO_x/TiO_2 catalysts are typically prepared by impregnation of soluble vanadium and tungsten oxide precursors

* Corresponding author.
E-mail address: iew0@lehigh.edu (I.E. Wachs).
[1] Present address: School of Electronic Information and Automation, Chongqing University of Technology, Chongqing 400030, China.

http://dx.doi.org/10.1016/j.apcatb.2016.04.022
0926-3373/

onto the titania support. The supported vanadia phase consists of mono-oxo surface VO_4 species (O = V(—O—Ti)$_3$) that oligomerize with increasing surface vanadia coverage [24–27] and also form crystalline V_2O_5 nanoparticles (NPs) when monolayer coverage is exceeded [24–27]. The supported tungsten oxide phase consists of mono-oxo surface WO_5 species (O = W(—O—Ti)$_4$) that also oligomerize with surface tungsta coverage [24] and can form crystalline WO_3 NPs above monolayer coverage.

At low total vanadia and tungsta coverages on TiO_2, the surface structures of vanadium and tungsten oxides are not influenced by each other [24]. At higher vanadia loadings, moderately distorted surface vanadia species become more abundant with increasing tungsta loadings [24]. This finding is thought to partially account for the promotional effect of tungsta, since such moderately distorted vanadia species are generally believed to be responsible for the exceptional SCR performance of vanadium-based catalysts [1–9,16]. It has recently been proposed that tungsta may cause formation of a single surface oxide phase of an intimate mixture of surface tungsta and vanadia instead of promoting surface vanadium oxide island formation [28]. The distribution of the surface VO_4 and WO_5 sites on the TiO_2 support, however, is still an unresolved issue since direct observation has not been reported in the literature.

Syntheses of supported VO_x-WO_x/TiO_2 catalysts have also been reported *via* multiple impregnation techniques [29–31]. Although differences in the reducibility of the catalysts (by hydrogen temperature-programmed reduction) were found, the SCR activity of the resulting catalysts was independent of the order of introduction of vanadium and tungsten oxide precursors [29,30]. Supported WO_x/TiO_2 catalysts prepared by a sol-gel method have been reported to exhibit good activity at high operating temperatures (350–600 °C) [32]. In other studies, the dispersion of tungsten oxide on TiO_2 supports was found to be higher when these catalysts were prepared by chemical methods (flame spraying [33] or sequential impregnation [29,30,34,35]) rather than mechanical techniques such as mechanical ball milling [36]. Co-precipitated WO_3-TiO_2 catalysts prepared from titanyl sulfate and ammonium paratungstate have been reported to possess greater thermal durability than the impregnated and grafted catalysts [8]. In contrast, other researchers have concluded that the choice of the TiO_2 precursor, titanium oxyhydroxide or TiO_2 powder, does not affect the development of the catalyst structure, surface acidity or its catalytic performance for 2-propanol dehydration and *n*-hexane isomerization [37]. Some studies have proposed that tungsten oxide may also be present in the titania interlayer spaces in the co-precipitated catalysts, but supporting evidence has not been provided [1,2,38,39].

According to the prior studies, the catalyst preparation method is a critical factor in determining the interaction between the active vanadium and tungsten oxide components and the titania support. Therefore, it is important to carefully compare the characterization and activity of catalysts prepared by different synthesis methods. In the present paper, the structural, physico-chemical properties and reactivity of V_2O_5-WO_3/TiO_2 catalysts prepared by co-precipitation of $TiO(OH)_2$ with ammonium metatungstate and ammonium metavanadate are compared with those of the catalysts prepared by the conventional impregnation method. The new findings reveal that the synthesis methods affect both the textural and chemical properties of the V_2O_5-WO_3/TiO_2 catalysts for the SCR reaction.

2. Experimental

2.1. Catalyst preparation

Metatitanic acid was precipitated from titanium isopropoxide (Ti(O-*i*-Pr)$_4$, Alfa Aesar, 99.999%) by addition of deionized water (molar ratio water/titanium isopropoxide = 110). After 60 min of stirring, the solution was filtered. The powder was washed and finally dried at 120 °C for 6 h. The powder thus obtained was then added the appropriate amount of deionized water to obtain a $TiO(OH)_2$ slurry with a concentration of 2 mol/L. Afterwards aqueous solutions of ammonium metatungstate (Pfaltz & Bauer, 99.5% purity; 0.06 M) and ammonium metavanadate (Aldrich; 0.35 M) were poured into the $TiO(OH)_2$ suspension, respectively. Into this mixed suspension, a solution of aqueous ammonia (Fisher Scientific) was gradually added dropwise with stirring to obtain the desired pH value of approximately 8 to produce a co-precipitate gel. Water was removed from the gel by evaporation in a water bath. Each sample was dried at 120 °C overnight, and then calcined at 550 °C (heating rate 1 °C/min) for 4 h in an atmosphere of air. This same procedure, with the exclusion of ammonium metavanadate, was followed to make the sample of co-precipitated 5% WO_3-TiO_2.

For comparison, supported VO_x-WO_x/TiO_2 catalysts were prepared by the incipient wetness impregnation method. The appropriate volume of an aqueous solution of ammonium metatungstate (0.06 M) or ammonium metavanadate (0.35 M) was poured onto TiO_2 (Degussa/Evonik, P-25, ~55 m^2/g, predominantly TiO_2(anatase)). After 30 min of thorough mixing, the sample was dried overnight under ambient conditions. Subsequently, this impregnation was repeated with the second active catalyst component, and the sample(s) dried overnight under ambient conditions. Finally, the catalysts were dried in flowing air (100 cm^3/min) at 120 °C for 2 h and then calcined in flowing air at 550 °C (heating rate 1 °C/min) for 4 h. This same procedure, with the exclusion of ammonium metavanadate, was followed to make the sample of impregnated supported 5% WO_x/TiO_2. The impregnated supported 1% VO_x/TiO_2 was prepared from vanadyl triisopropoxide by a standard procedure [40].

The V_2O_5-WO_3/TiO_2 catalysts prepared by co-precipitation and incipient wetness impregnation are denoted as *a*V*b*WTi(C), and *a*V*b*WTi(I), respectively, where a and b represent the loadings of V_2O_5(wt.%) and WO_3(wt.%), and (C) and (I) denote co-precipitation and incipient wetness impregnation. For example, 1V5WTi(C) means the V_2O_5-WO_3/TiO_2 catalyst with a V_2O_5 loading of 1 wt.% and WO_3 loading of 5 wt.%, prepared by the co-precipitation method.

2.2. Catalyst characterization

2.2.1. BET-specific surface area measurement

BET surface areas of the samples were determined from adsorption-desorption isotherms of N_2 at −196 °C using a Micromeritics ASAP 2020 apparatus. Typically, 0.200–0.300 g sample was used for each measurement. Each sample was outgassed under vacuum at 300 °C for 6 h prior to N_2 adsorption. The total pore volume, average pore diameters and pore size distributions were obtained from the N_2 adsorption branches of isotherms using the Barret-Joyner-Halenda (BJH) method.

2.2.2. XRD

XRD spectra was measured with a Rigaku Miniflex II diffractometer using CuK-α radiation (1.5418 Å). Full scans of 5–90° (2-theta) were measured with a scan rate of 1 deg/min. The major peak scans of 23–26° (2-theta) were measured with a scan rate of 0.1 deg/min.

2.2.3. HS-LEIS

The outermost surface information was analyzed by Qtac^{100} HS-LEIS spectrometer (ION-TOF) equipped with a highly sensitive double toroidal analyzer. The equipment provides 3000-fold higher sensitivity than conventional LEIS spectrometers, allowing for quantitative static depth profiling. Prior to the measurements,

the samples were dehydrated in static O_2 at 400 °C for 1 h in a preparation chamber connected to the spectrometer. After dehydration, the preparation chamber was evacuated and the samples were directly transferred to the main UHV chamber for the measurements. The HS-LEIS spectra were collected using 1.0 KeV He^+ as ion sources. For depth profiling, the surface was sputtered with 3.0 KeV Ar^+, each sputter and measurement cycle yield of 1×10^{15} ions/cm^2 corresponding to ~1 surface layer (0.2 nm).

2.2.4. Raman spectroscopy

The molecular structure of the catalysts was determined by Raman spectroscopy with a visible (532 nm) laser excitation on a single stage Horiba-Jobin Yvon Laboratory Ram-HR Raman spectrometer with a confocal microscope (Olympus BX-30) and a notch filter (Kaiser Super Notch). The visible excitation was generated by a Nd-YAG double diode pumped laser (Coherent Compass 315M-150, output power of 150 mW with power at the sample of 10 mW). The scattered photons were directed into a single monochromator and focused onto a UV-sensitive liquid N_2 cooled CCD detector (Horiba-Jobin Yvon CCD-3000 V) with a spectral resolution of ~1 cm^{-1} for the given parameters. The catalysts were dehydrated in an *in situ* cell (Linkam CCR1000) by flowing 10% O_2/Ar (Airgas, 10%O_2/Ar, 25 mL/min) at 450 °C for 1 h, and then cooled under flowing 10% O_2/Ar to 120 °C to ensure that the catalyst surface was free of moisture before the spectra were collected.

2.2.5. Infrared spectroscopy

The *in situ* IR experiments were performed on a Thermo NICOLET 8700 FTIR spectrometer equipped with a Harrick Praying Mantis Attachment (Model DRA-2) for diffuse reflectance spectroscopy and a high sensitive mercury-cadmium-telluride (MCT-A) detector. Powder samples were loaded into a Harrick Scientific cell (HVC-DRP4) which directly connected to a purging and adsorption gas control system. The temperature of the reaction chamber was controlled by a Harrick ATC Temperature Controller unit.

Catalysts were dehydrated by heating to 450 °C (heating rate of 10 °C/min) and holding at 450 °C for 1 h under flowing 10% O_2/Ar (30 mL/min). The *in situ* IR spectra in the overtone region of the dehydrated samples were collected after cooling the catalysts to 110 °C under flowing 10% O_2/Ar. Subsequently at 110 °C, 10% O_2/Ar was replaced by flowing Ar (30 mL/min; 20 min) and then by flowing 1.5% NH_3/He (30 mL/min; 30 min). Physisorbed NH_3 was removed by flowing Ar (30 mL/min; 30 min). The integrated *in situ* IR bands of the surface NH_3* and NH_4^+** species were normalized against the IR band of the TiO_2 support at ~800 cm^{-1}.

For the $H_2{}^{18}O$ isotope exchange experiments, *in situ* IR spectra were collected with a Thermo Nicolet Nexus 670 spectrometer equipped with a diffuse reflectance cell (HC-900, Pike Technologies). The sample was pretreated in flowing 5% O_2/He (25 mL/min) at 450 °C for 1 h. An *in situ* IR spectrum of the unlabeled catalyst was collected after cooling to 120 °C in flowing 5% O_2/He (25 mL/min). The sample was then heated to 400 °C under flowing 5% O_2/He (25 mL/min). A background spectrum was obtained before the sample was exposed to $H_2{}^{18}O$/He (15 mL/min He bubbling through a $H_2{}^{18}O$ saturator at room temperature) at 400 °C for 1 h. Time-resolved spectra were collected during the isotope exchange process. The sample was further purged with He (25 mL/min) at for 90 min before cooling to 120 °C under flowing He and the spectrum of the isotope exchanged catalyst was then collected.

2.2.6. Temperature-programmed surface reaction (TPSR) spectroscopy

The surface chemistry and reactivity of the supported tungsten oxide catalysts were chemically probed by NH_3 TPSR spectroscopy, using an Altamira AMI-200 spectroscope equipped with a Dycor Dymaxion DME200MS online quadrupole mass spectrometer. Typically, ~160 mg of catalyst was loaded into a U-type quartz tube and initially treated in flowing 10%O_2/Ar to 480 °C (30 mL/min; heating rate of 10 °C/min) for 60 min to remove any possible adsorbed organic impurities and to dehydrate the sample. To ensure that the surface MO_x species remained in the fully oxidized state, the pretreated samples were cooled to 60 °C under flowing 10% O_2/Ar at which time the gas stream was switched to Ar (Airgas, ultra-high purity. 30 mL/min) and held for 30 min to flush out any residual gas-phase O_2 and to remove any physically adsorbed O_2 and background gases. After the O_2 treatment, two different experiments were performed. For first type of experiment, a SCR reaction mixture was introduced (35 mL/min of NH_3/He (2000 ppm; Airgas, ultra-high purity), 35 mL/min of NO/He (2000 ppm; Airgas, ultra-high purity), 5 mL/min of 5% O_2/He (Airgas, ultra-high purity) and 5 mL/min of Ar (Airgas, ultra-high purity), then the sample was heated to 500 °C at a rate of 10 °C/min. For the second type of experiment, ammonia was initially adsorbed at 60 °C by flowing 30 mL/min of NH_3/He (2000 ppm)) for 30 min and the system was subsequently purged with flowing Ar (30 mL/min) for another 30 min to remove any physically adsorbed ammonia. The gas stream was then switched to either 30 mL/min of NO/He (2000 ppm) or a mixture of 35 mL/min of NO/He (2000 ppm) and 5 mL/min of 5% O_2/He. After flowing either the NO/He or NO/O_2/He for 10 min at 60 °C, the catalyst was heated at a constant heating rate (5 °C/min) to 480 °C and held at 480 °C for 30 min.

The gases exiting the quartz tube fixed-bed reactor were analyzed with the online mass spectrometer as a function of catalyst temperature. The following m/z ratios were employed for the identification of the desorption gases: N_2 (m/z = 28), H_2O (m/z = 18), NH_3 (m/z = 17), NO (m/z = 30), N_2O (m/z = 44) and NO_2 (m/z = 46). The NH_3 signal was corrected for the cracking contribution of H_2O in the MS m/z = 17 signal.

2.2.7. Steady-state SCR reaction

The steady-state SCR reaction was performed on an Altamira AMI-200 fixed-bed reactor equipped with a Dycor Dymaxion DME200MS online quadrupole mass spectrometer. About 30 mg of catalyst was loaded into a U-type quartz fixed-bed reactor for the reaction studies and held in place by quartz wool. The catalyst was initially treated with 10% O_2/Ar at 500 °C for 1 h to remove any possible adsorbed organic impurities, adsorbed moisture and to ensure that the surface vanadium and tungsten oxide sites are in the fully oxidized state. The reactor system was then flushed with He for 10 min, after which a SCR reaction mixture was introduced (35 mL/min of NH_3/He (2000 ppm), 35 mL/min of NO/He (2000 ppm), 5 mL/min of 5% O_2/He and 5 mL/min of Ar). The SCR reaction was performed at several temperatures for 2 h at each temperature to ensure that steady-state reaction conditions were achieved. The gases exiting the quartz tubular reactor were analyzed with the online mass spectrometer. The following m/z ratios were employed for the identification of the exiting gases: O_2 (m/z = 32), N_2 (m/z = 28), NH_3 (m/z = 17), NO (m/z = 30), NO_2 (m/z = 46) and N_2O (m/z = 44). The MS signals of the reactants and products were calibrated and normalized against the He signal. The NO conversions at 265 °C were typically below 10% with the exception of the highly active 1V5W/Ti(C) catalyst that yielded much more than 10% conversion above 220 °C (see Table S2).

3. Results

3.1. Textural properties

The BET surface area, BJH adsorption pore volume and average pore diameter of the investigated samples are summarized

Table 1
BET surface area, Barrett Joiner Halenda (BJH) pore volume, and pore distribution for the co-precipitated and incipient wetness analogs for 5%WO_3-TiO_2, 1% V_2O_5-TiO_2 and 1%V_2O_5-5%WO_3-TiO_2 catalysts.

Catalyst[a]	Surface area (m^2/g)	Pore volume (cm^3/g)	Pore size (nm)	Surface density W/V (atom/nm^2)
5WTi(C)	84	0.20	8.5	1.5
5WTi(I)	53	0.43	30.2	2.4
1VTi(C)	41	0.14	12.2	0.8
1VTi(I)	40	0.22	12.0	0.8
1V5WTi(C)	53	0.16	10.7	0.6 V; 2.4 W
1V5WTi(I)	54	0.34	24.4	0.6 V; 2.4 W

[a] All catalysts calcined at 550 °C.

in Table 1. The highest surface areas are found for the 5WTi catalysts with the co-precipitated catalyst possessing ~1.6× higher surface area than the impregnated catalyst. The surface areas of the 1VTi catalysts are the same for the co-precipitated and impregnated catalysts, but lower than the WTi catalysts. The BET values of the 1V5WTi catalysts are also the same for both synthesis methods and ~1.3× higher than the 1VTi catalysts reflecting the surface area stabilization of the tungsten oxide. The co-precipitated catalysts generally possess lower pore volume and smaller pores as the analogous impregnated catalysts. The pore size distribution indicates that the co-precipitated catalysts primarily consist of mesopores [41]. Although the larger pore volume of the incipient wetness catalysts is beneficial in minimizing mass transfer limitations, the corresponding larger pore diameter and volume can lead to greater catalyst deactivation from sintering [3].

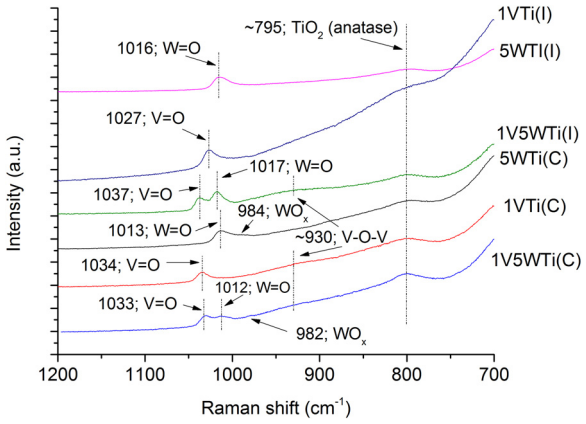

Fig. 1. *In situ* Raman (532 nm) spectra of dehydrated co-precipitated and impregnated VWTi catalysts.

3.2. XRD and HS-LEIS

The XRD diffractograms are given in Figs. S1 and S2 and reveal that TiO_2(P-25)-containing catalysts mainly consist of the anatase phase, but also contain some rutile phase. The co-precipitated TiO_2(C)-containing catalysts are also dominated by the anatase phase without rutile, but also possess some brookite phase and $H_2Ti_3O_7$. The constant position of the TiO_2(anatase) peaks for the coprecipitated catalysts reveals that there is no evidence for formation of V-Ti and W-Ti oxide solid solutions. HS-LEIS surface analysis confirms that the W/Ti and V/Ti ratios are essentially the same for the co-precipitated and model impregnated catalysts indicating surface segregation of the V and W oxides on the titania support. (Figs. S3 and S4). Depth profiling of the P-25 supported and co-precipitated VTi catalysts showed that the values of the V/Ti ratios decreased rapidly from ~0.2 at the catalyst surface to ~0.02 at 1.0 nm depth. Similarly, depth profiling of the P-25 supported and co-precipitated VWTi catalysts showed that the values of the V/Ti ratios decreased from ~0.2 at the surface to ~0.05 at 1.0 nm, and that the values of the W/Ti ratios declined from ~1.2 at the surface to ~0.5 at 1.0 nm. Both sets of results are consistent with surface segregation of the V and W oxides. The broader XRD peaks for the co-precipitated catalysts reflect the greater disorder of the co-precipitated catalysts relative to the impregnated catalysts (see Table S1).

3.3. In situ *Raman spectroscopy*

The Raman spectra of the titania supports for 1V5WTi(I) and 1V5WTi(C) are dominated by that of crystalline TiO_2 (anatase) at ~397, ~514 and ~638 cm^{-1} [42,43] and presented in the Supplemental information Section as Fig. S5. Some TiO_2 (brookite) phase, Raman bands at ~320 and ~244 cm^{-1} [42,43], is also observed for the co-precipitated catalyst samples since brookite is formed during the formation and hydrolysis of $TiO(OH)_2$. Bands from TiO_2 (rutile) at ~445 and ~610 cm^{-1} are not evident in any of the spectra [42].

The *in situ* Raman spectra for the dehydrated catalysts are shown in Fig. 1. Note that the TiO_2 (anatase) support gives rise to a weak second-order feature at ~795 cm^{-1} [44,45]. The symmetric stretch of the terminal V = O vibration at 1027–1037 cm^{-1} for both 1VTi(I) and 1VTi(C) is associated with oligomeric surface mono-oxo O = VO_3 sites [10,24]. The broad band centered at ~930 cm^{-1} is assigned to the bridging V-O-Ti anchoring bonds [46]. Raman bands from crystalline V_2O_5 nanoparticles, at ~995 cm^{-1}, are not present in any of the catalysts indicating complete dispersion of vanadia on the TiO_2 support [10,16,24]. Although the surface V = O symmetric stretch vibrations do not shift for the co-precipitated catalysts when tungsten oxide is added, the surface V = O bands are slightly blue shifted from 1027 to 1037 cm^{-1} upon tungsten oxide addition for the impregnated 1VTi(I) catalyst reflecting formation of larger surface VO_4 oligomers in the presence of the surface tungsten oxide species [47]. The terminal W = O vibration at ~1010–1017 cm^{-1} is associated with surface mono-oxo O = WO_4 sites [15,24,33,48,49]. The slight blue shift of the W = O band for the impregnated catalysts compared to the co-precipitated catalysts suggests that the surface WO_5 sites are slightly more polymerized for the impregnated catalyst. The co-precipitated catalysts also contain a new weak Raman band at ~982–984 cm^{-1} that is assigned to a second surface mono-oxo O = WO_4 site anchored at surface defects of the TiO_2 support based on similar behavior for surface vanadia on defective CeO_2 [50]. Raman bands from crystalline WO_3 nanoparticles, at ~805 cm^{-1}, are not present in any of the catalysts indicating complete dispersion of tungsten oxide on the TiO_2 support [10,16,24]. The Raman spectra demonstrate that the supported tungsten oxide and vanadium oxide phases are completely dispersed on the titania support for both the co-precipitated and impregnated catalysts.

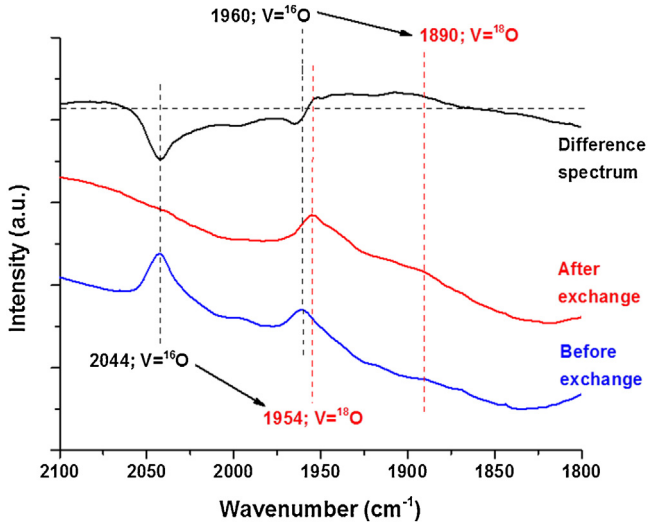

Fig. 2. Absorbance *in situ* IR spectra of 1VTi(C) catalyst before and after isotopic exchange and difference IR spectrum after isotopic exchange. Absorbance = log(1/I), Difference = $\log(I_{before}/I_{after})$.

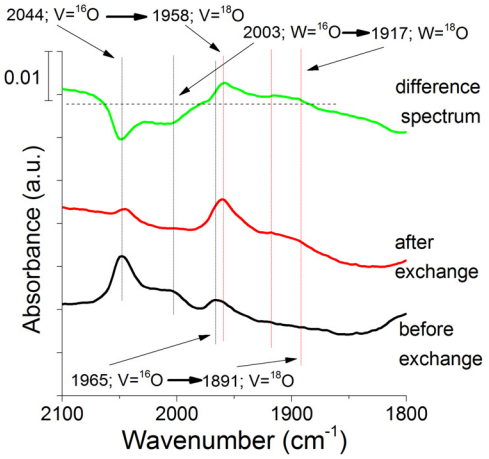

Fig. 3. Absorbance *in situ* IR spectra of 1V5WTi(C) catalyst before and after isotopic exchange and difference IR spectrum after isotopic exchange. Absorbance = log(1/I), Difference = $\log(I_{before}/I_{after})$.

3.4. In situ *IR spectroscopy*

The *in situ* IR spectra of the co-precipitated and impregnated dehydrated catalysts in the overtone region are shown in Fig. S6 and complement the above Raman spectra. The presence of only single V=O and W=O overtone bands at ~2040–2050 and 2017–2020 cm^{-1} for both the impregnated and co-precipitated 1VTi and 5WTi catalysts confirm the mono-oxo structure of the surface VO_4 and WO_5 sites, respectively, from IR and Raman vibrational spectroscopy selection rules [51]. The IR overtone band for the second surface WO_5 species for the 5WTi (C) catalyst is more evident at ~1993 cm^{-1}. The appearance of this W=O vibration at the same values for Raman (overtone expected at ~1990 cm^{-1}) and IR (overtone at 1993 cm^{-1}) indicates that this second surface WO_5 site also has mono-oxo $O=WO_4$ coordination from Raman and IR selection rules. The tungsten oxide IR overtone bands are too broad and overlap for the 1V5WTi(C) catalyst to separate the contributions of each tungsten oxide site. The apparent greater sensitivity of the IR overtone spectrum also detects a new band at 1960–1965 cm^{-1} for the 1VTi(C) and 1V5WTi(C) catalysts that is not present for the 1VTi(I) and 1V5WTi(I) catalysts. This new IR band is also assigned to a second surface mono-oxo $O=VO_3$ site anchored at surface defects of the TiO_2 support based on similar behavior for surface vanadia on defective CeO_2 [50] and its absence for the low defect TiO_2 support used to synthesize the impregnated catalysts [52]. Additional insights about the nature of the surface vanadia and tungsta species on the TiO_2 support were provided from *in situ* IR spectra of ^{18}O-^{16}O exchanged catalysts.

The *in situ* IR spectra of the dehydrated 1VTi(C) catalyst before and after ^{18}O-^{16}O exchange, as well as their difference spectrum, are presented in Fig. 2. Prior to exchange, the two vanadia IR overtone bands at 2044 and 1960 cm^{-1} are present from the symmetric stretch of terminal $V=^{16}O$ bonds from surface VO_4 sites on less defective and highly defective TiO_2 patches, respectively. Upon ^{18}O-^{16}O exchange, the symmetric stretch at 2044 cm^{-1} ($V=^{16}O$) shifts to 1954 cm^{-1} ($V=^{18}O$) and the symmetric stretch at 1960 cm^{-1} ($V=^{16}O$) shifts to 1890 cm^{-1} ($V=^{18}O$). The broader IR bands after the $H_2{}^{18}O$ exchange are related to the presence of residual moisture in the cell after the water exchange experiment. The efficient oxygen exchange further confirms the surface nature of the vanadia sites.

The *in situ* IR spectra of the ^{16}O-^{18}O exchanged 5WTi(C) catalyst prepared at a pH = 5 are not shown for brevity and upon oxygen exchange the overtone W=O symmetric stretch at 2013 cm^{-1} shifts to 1907 cm^{-1} and the W=O symmetric stretch at 2003 cm^{-1} shifts to 1890 cm^{-1}. The absence of dioxo $^{16}O=W=^{18}O$ bands further confirms the mono-oxo W=O nature of the surface tungsten oxide species and the rapid oxygen exchange demonstrates that the tungsten oxide species are present on the surface of the TiO_2(C) support.

The *in situ* IR spectra of the ^{16}O-^{18}O exchanged 1V5WTi(C) catalyst are given in Fig. 3 and are almost a combination of the results of the individual 1VTi(C) and 5WTi(C) catalysts. The individual overtone V=O and W=O symmetric stretches are minimally perturbed by the presence of the other metal oxide (*e.g.*, VO_4 minimally affects WO_5 and WO_5 minimally affects VO_4). The IR spectra are dominated by the stronger signals from the surface vanadia sites than the surface tungsta sites. The rapid oxygen exchange demonstrates that the vanadia and tungsten oxide are indeed present on the surface of the TiO_2(C) support for the 1V5WTi(C) catalyst (see time-resolved spectra in Fig. S7).

3.5. *Surface acidity*

The surface acidity of VWTi catalysts is known to significantly impact the NO/NH_3 SCR reaction and is typically chemically probed by ammonia chemisorption [53–55]. The *in situ* IR spectra before and after chemisorption of ammonia on the series of dehydrated catalysts are presented in Figs. S8 and S9. Chemisorption of ammonia on the VWTi catalysts significantly diminishes the intensity of the IR bands of the surface hydroxyls and reflects the direct interaction of ammonia with the surface hydroxyls. The IR bands at 1180 and 1603 cm^{-1} correspond to the symmetric and asymmetric bending vibrations, respectively, of surface NH_3* chemisorbed on Lewis acid sites [2,17,18,53–55]. The IR band at 1419 cm^{-1} is from the asymmetric bending vibration of surface $NH_4{}^{+}$* chemisorbed on Brønsted acid sites [17,53–55]. The related symmetric stretch of the surface $NH_4{}^{+}$* chemisorbed on Brønsted acid sites, reported to be at 1660 cm^{-1} [56], is not apparent in the IR spectra. The surface NH_3* species bound to Lewis acid sites also vibrate at 3100–3400 cm^{-1} and the surface $NH_4{}^{+}$* species also vibrate at 1430 cm^{-1} [53]. The IR bands at 3161/3257 and 3346/3382 cm^{-1} are from N—H stretching modes of surface NH_3* coordinated to Lewis acid sites [56].

It is well known that TiO_2 contains only weak Lewis acid sites and that the addition of surface transition metal oxides introduces Brønsted acid sites [57]. All the WO_x- and VO_x-containing titania catalysts contain both surface Brønsted and Lewis acid sites

Table 2
IR analysis of surface Brønsted (1419 cm^{-1}) and Lewis acid (1603 cm^{-1}) sites probed with ammonia adsorption at 100 °C.

Catalyst[a]	Ratio of B/L sites	Ratio of Bronsted (1419 cm^{-1}) sites/TiO_2 (~800 cm^{-1}) x 10^2	Ratio of Lewis (1603 cm^{-1}) sites/TiO_2 (~800 cm^{-1}) x 10^2
5WTi(C)	0.97	3.6	3.7
1VTi(C)	1.4	4.2	3.0
1V5WTi(C)	2.7	6.7	2.5
5WTi(I)	1.2	4.0	3.3
1V5WTi(I)	3.9	10.0	2.6

[a] All catalysts calcined at 550 °C.

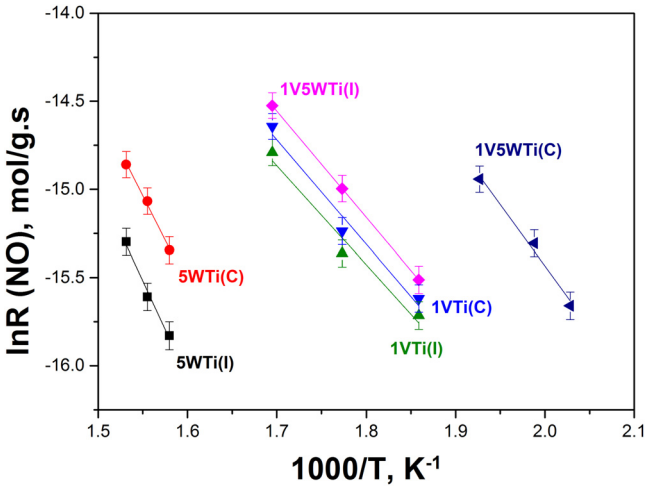

Fig. 4. Arrhenius plot for steady-state NO/NH_3 SCR kinetics.

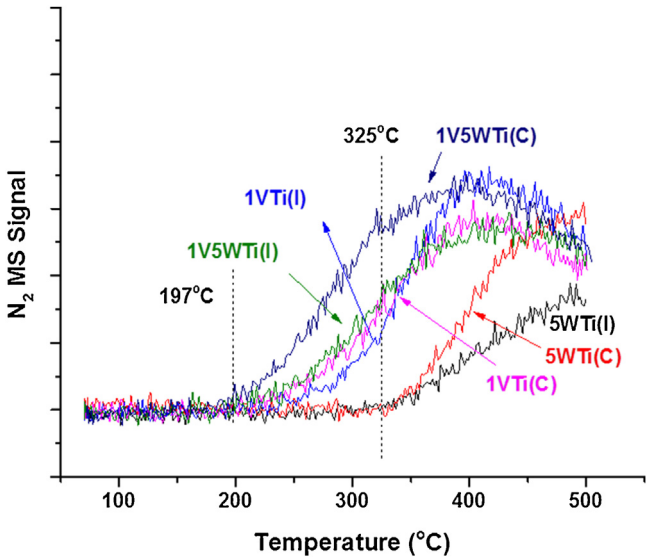

Fig. 5. Normalized MS signals for evolution of N_2 during NO/NH_3/O_2 SCR-TPSR for the 5WTi, 1VTi and 1V5WTi catalysts.

as shown in Table 2. For the WO_x-containing catalysts, both catalyst types have comparable amounts of surface Brønsted and Lewis acid sites. The addition of vanadia to the WTi catalysts markedly increases the Brønsted/Lewis acid site ratios. The ratios of Brønsted/Lewis acid sites for the VWTi catalysts are also summarized in Table 2. The Brønsted/Lewis acid site ratios are higher for the impregnated catalysts than the co-precipitated catalysts.

3.6. Steady-state SCR kinetics

The steady-state kinetics for the NO/NH_3/O_2 SCR reaction by the 5WTi, 1VTi and 1V5WTi catalysts prepared by co-precipitation and impregnation are presented in Fig. 4 as Arrhenius plots and additional information is provided in Tables S2 and S3. Neither N_2O or NO_2 products were formed under the present SCR reaction conditions. The 5WTi catalysts exhibit the lowest SCR activity with the 5WTi(C) catalyst more active than the 5WTi(I) catalyst. The 1VTi catalysts are much more active than the 5WTi catalysts, reflecting the importance of redox vanadia sites upon the SCR reaction, with the 1VTi(C) catalyst slightly more active than the 1VTi(I) catalyst even with the same surface area. The combination of vanadium and tungsten oxides further increased the SCR activity. For the 1V5WTi catalysts, the presence of both oxides modestly increased the activity of the 1V5WTi(I) catalyst but dramatically increased the activity of the 1V5WTi(C) catalyst even with the same surface area. Only the 1V5WTi(C) catalyst yielded high NO conversions (10% at 220 °C, 14% at 230 °C and 21% at 246 °C). The steady-state TOF values for the series of catalysts at 265 °C follow the order 1V5WTi(C) $(4.8 \times 10^{-3}/s) >$ 1V5WTi(I) $(1.7 \times 10^{-3}/s) \sim$ 1VTi(C) $(1.5 \times 10^{-3}/s) \sim$ 1VTi(I) $(1.4 \times 10^{-3}/s) \gg$ 5WTi(C) $(6.2 \times 10^{-5}/s) >$ 5WTi(I) $(2.9 \times 10^{-5}/s)$. The surface vanadia sites were taken as the active sites for all V-containing catalysts and the surface tungsten oxide sites were taken as the active sites for the WTi catalysts (see below for additional justification). For all analogous catalysts with the same composition, the co-precipitated catalysts were always found to be more active than the impregnated catalysts.

The steady-state reaction orders were not determined in the present study since it is well known that the SCR kinetics over VWTi catalysts is 1st-order in NO and zero-order in both NH_3 and O_2 [58,59]. The zero-order dependence on the ammonia partial pressure reflects the high surface coverage of ammonia on the catalyst during reaction and the zero-order in O_2 reflects the participation of surface lattice oxygen rather gas phase molecular O_2 in the rate-determining-step of the SCR reaction *via* a Mars-van Krevelen mechanism.

The activation energies for the SCR reaction were ~83–91 kJ/mol for the WTi catalysts, with the higher value corresponding to the 5WTi(I) catalyst, and decreased to ~50 kJ/mol for the V-containing catalysts (see Table S3 in SI). This indicates that the surface vanadia sites dominate the SCR reaction kinetics. It also suggests that differences in SCR activity are mostly affected by variation in the pre-exponential factor that is highest for the 1V5WTi(C) catalyst, which is more than 6x larger than for the corresponding 1V5WTi(I) catalyst.

3.7. NO/NH_3/O_2 SCR temperature-programmed surface reaction (TPSR) spectroscopy

Additional fundamental insights about the NO/NH_3/O_2 SCR reaction by the 1WTi, 1VTi and 1V5WTi catalysts were provided from TPSR experiments (Fig. 5). Both 5WTi catalysts initiate the SCR

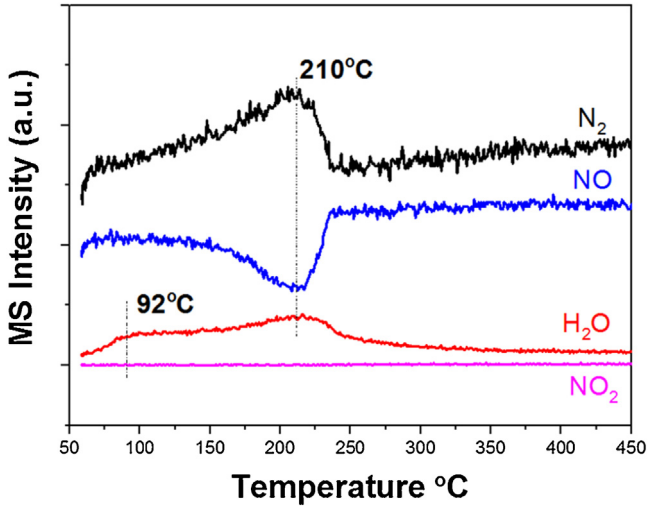

Fig. 6. NO/O_2-TPSR with chemisorbed ammonia on the 1V5WTi(C) catalyst.

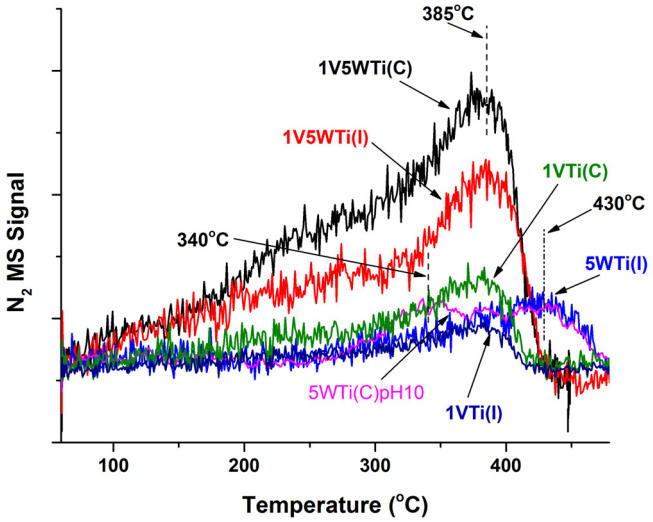

Fig. 7. Comparison of NO/NH_3 SCR-TPSR spectra for N_2 evolution for 5WTi(I), 5WTi(C) 1VTi(I), 1V5WTi(I), 1VTi(C), and 1V5WTi(C) catalysts. The experiments were conducted by first chemisorbing ammonia on the catalyst and heating the catalyst in flowing NO/He.

reaction at ~325 °C with N_2 formation increasing faster for 5WTi(C) than 5WTi(I). The V-containing catalysts initiate the SCR reaction at ~200 °C reflecting the dominant kinetic role of the vanadia sites for this reaction. The evolution of N_2 from the 1VTi(C) catalyst is slightly greater than that for the 1VTi(I) catalyst. Addition of tungsten oxide to the 1VTi(I) catalyst modestly increases the evolution of N_2, but tungsten oxide addition to 1VTi(C) significantly increases N_2 evolution. The surface tungsten oxide sites do not directly participate in the SCR reaction between 200 and 325 °C since the SCR reaction only takes place on the 5WTi catalysts above 325 °C. All the co-precipitated catalysts are more active for the SCR reaction than their analogous impregnated catalysts.

The surface chemistry of the SCR reaction was further probed with TPSR where the 1V5WTi(C) catalyst was initially saturated with a monolayer of ammonia and then heated in flowing NO/O_2/He are presented in Fig. 6. Both NO_2 and N_2O products were not formed as reaction products under the TPSR experimental conditions. The initial reaction product is H_2O indicating breaking of some N—H bonds upon adsorption of ammonia and exposure to NO/O_2 in the ~100 °C region. The desorption of H_2O is not from background condensed moisture on the catalyst since D_2O was also formed at this temperature when ND_3 is employed. The SCR reaction initiates at ~100 °C with the evolution of N_2 and the consumption of NO. The surface ammonia species are completely consumed by ~240 °C, with a Tp of ~210 °C for N_2 evolution. When the TPSR experiment is repeated in the absence of gas phase molecular O_2, the SCR reaction still proceeds but shifts the Tp to ~350 °C (see Fig. S10 in SI). The fact that the SCR reaction can take place in the absence of gas phase molecular O_2 demonstrates that oxygen from the redox surface vanadia sites is able to perform the SCR reaction. The significant shift of T_p from 210 to 350 °C indicates that the surface vanadia sites present in the V^{+5} oxidation state are much more active than partially reduced surface vanadia sites for the SCR reaction.

The evolution of N_2 during TPSR in flowing NO/He following ammonia adsorption was examined to provide information about the amounts of reactive surface ammonia present on the different catalysts, which is proportional to the area under the N_2 evolution TPSR curves and is presented in Fig. 7. The absence of gas phase molecular O_2 is not critical for this experiment since the adsorbed ammonia is almost completely converted to N_2 in both the presence and absence of gas phase O_2 by the oxygen supplied by the surface VO_x sites. The amount of N_2 produced varies as 1V5WTi(C) (1.5x) > 1V5WTi(I) (1.0x) > 1VTi(C) (0.4x) > 5WTi(C) (0.3x) > 5WTi(I) (0.2x) ~ 1VTi(I) (0.2x). Although the co-precipitated 1V5WTi(C) and impregnated 1V5WTi(I) catalysts possess the same composition and surface area, the co-precipitated catalyst forms ~50% more N_2 than the impregnated catalyst reflecting the presence of more reactive surface ammonia species on the co-precipitated catalyst. This difference is not related to the small desorption of unreacted ammonia since the co-precipitated catalysts also desorb more ammonia than the impregnated catalyst (see Fig. S11 in SI). Thus, the co-precipitated catalysts possess higher ammonia adsorption capacity than the impregnated catalysts.

4. Discussion

4.1. Molecular structures of dehydrated surface VO_x and WO_x species and their anchoring sites on the TiO_2 support

The impregnated 5WTi(I) and 1VT(I) catalysts on the TiO_2 (P-25) support, prepared at high temperatures (~1000–1100 °C [60]) that are expected to have a low density of surface defects, contain only one surface mono-oxo $O=WO_4$ site (Raman: ~1016 cm^{-1}; IR overtone: ~2020 cm^{-1}) and mono-oxo $O=VO_3$ site (Raman: ~1027 cm^{-1}; IR overtone: 2038 cm^{-1}), respectively. The impregnated 1V5WTi(I) catalyst contains one mono-oxo $O=WO_4$ site (Raman: 1017 cm^{-1}; IR overtone: 2020 cm^{-1}) and one mono-oxo $O=VO_3$ (Raman: ~1037 cm^{-1}; IR overtone: ~2053 cm^{-1}) site. The blue shift of the symmetric stretch of the V=O Raman vibration from 1027 to 1037 cm^{-1} reflects the further oligomerization of the surface VO_x sites by the addition of the surface WO_x sites [61].

The co-precipitated 5WTi(C) and 1VTi(C) catalysts, however, contain two distinct surface mono-oxo $O=WO_4$ sites (Raman: ~1013 and ~984 cm^{-1}: IR overtone: ~2017 and ~1992 cm^{-1}) and two distinct surface mono-oxo $O=VO_3$ sites (Raman: ~1034 cm^{-1}; IR overtones: ~2043 and ~1960 cm^{-1}). By comparison with the impregnated catalysts on the low defect TiO_2 (P-25) support, for the co-precipitated catalysts the surface $O=WO_4$ sites vibrating at ~1013 cm^{-1} and the surface $O=VO_3$ sites vibrating at 1034 cm^{-1} reside on patches of low surface defect density TiO_2. The new surface $O=WO_4$ sites vibrating at ~984 cm^{-1} (overtone at ~1992 cm^{-1}) and new surface $O=VO_3$ sites vibrating at ~1960 cm^{-1} reside on poorly ordered patches with higher surface defect density of the co-precipitated TiO_2 support based on similar behavior for surface vanadia on defective CeO_2 supports [50]. The higher defect density of the co-precipitated TiO_2 is related to its

lower calcination temperature during catalyst synthesis (~550 °C) that results in smaller and/or poorly ordered TiO_2(anatase) particles as shown by XRD. The Raman bands for the surface VO_x and WO_x sites are minimally perturbed by the presence of the second surface oxide for the co-precipitated 1V5WTi(C) catalyst.

In general, shifts of the symmetric stretches of surface O = WO_4 and O = VO_3 sites with surface coverage is associated with oligomerization of the surface MO_x sites [61,62]. This suggests that the new surface MO_x sites thought to be associated with surface defects of the TiO_2 support are shorter oligomers than the surface MO_x sites vibrating above 1000 cm^{-1}.

It is not possible to quantify the surface defects present on titania for the co-precipitated catalysts by chemical probes such as adsorption of molecular O_2 because a fraction of the defects is covered by the surface WO_x and VO_x sites. Unfortunately, unlike CeO_2 where there is a distinct defect phonon [50], there is no such detectable phonon for the co-precipitated catalysts.

An interesting finding for the co-precipitated catalysts is that almost all the VO_x and WO_x surface segregate onto the TiO_2 support upon calcination at elevated temperatures rather than forming solid solutions. The driving force for this phenomenon is the lower surface free energy of V = O (~8 $\gamma/10^{-6}$ J/cm^2) and W = O (~10 $\gamma/10^{-6}$ J/cm^2) functionalities than surface Ti-OH functionalities (~33 $\gamma/10^{-6}$ J/cm^2) [63] and the incompatibility of the V^{+5} and W^{+6} cations with the TiO_2(anatase) phase. Furthermore, the high calcination temperature provides the thermal kinetic energy for the surface diffusion of VO_x (~210 °C) and WO_x (~600 °C).

4.2. Surface acidity

The TiO_2 support only contains weak Lewis acid sites and introduction of surface O = VO_3 and O = WO_4 sites generates both strong Brønsted and Lewis acidity [2]. Both the impregnated and co-precipitated 5WTi catalysts contain comparable surface Brønsted and Lewis acid sites. The addition of VO_x to the 5WTi(I) and 5WTi(C) catalysts, however, decreases the number of surface Lewis acid sites and significantly increases the number of Brønsted acid sites. Although the number of surface Lewis acid sites are comparable for both catalysts, the number of Brønsted acid sites is ~50% greater for 1V5WTi(I) than 1V5WTi(C), which suggests that the new surface VO_x/WO_x sites and the surface titania defects on the co-precipitated catalyst are suppressing the population of Brønsted acid sites.

4.3. Structure-activity relationships for NO/NH_3 SCR by VWTi catalysts

The co-precipitated catalysts always exhibit higher NO/NH_3/O_2 SCR activity than the impregnated catalysts (1V5WTi(C) » 1V5WTi(I); 1VTi(C) > 1VTi(I); 5WTi(C) > 5WTi(I)). With the exception of the WTi catalysts, both the 1V5WTi(C)/1V5WTi(I) and 1VTi(C)/1VTi(I) catalyst sets contain the exact same surface areas. The only physical difference between the corresponding impregnated and co-precipitated catalysts is the presence of new surface WO_x and VO_x sites ascribed to the presence of surface defects on the co-precipitated TiO_2 support. The presence of the new surface sites and the associated titania surface defects enhance the ammonia adsorption capacity of the co-precipitated catalysts, as shown from TPSR. The steady-state kinetics reveal that all the V-containing catalysts exhibit similar SCR activation energy values and the kinetics mainly differ in their pre-exponential factor values (a factor of ~18 from 4.9 to 89 × 10^{-3} mol/g·s). This kinetic trend is also reflected in the SCR TOF values at 265 °C by variation from 1.4 to 4.8 × 10^{-3}/s (a factor of ~3.5x).

The mono-oxo surface WO_5 sites do not perform the NO/NH_3/O_2 SCR reaction below 325 °C, which indicates that the SCR reaction is being performed by the mono-oxo surface VO_4 sites below 325 °C. This implicates the surface WO_5 sites as only being involved in chemisorption of ammonia below 325 °C for 5WTi(I) and 5WTi(C) catalysts.

The mono-oxo surface VO_4 sites are the catalytic active sites and dominate the NO/NH_3/O_2 SCR reaction kinetics as reflected in the very similar activation energy values and initiation of the SCR reaction at ~200 °C for all the V-containing catalysts. The SCR kinetics for the 1VTi(C) and 1VTi(I) are very similar with Ea of 49 and 47 kJ/mol, respectively, and pre-exponential factors of 4.9 × 10^{-3} and 9.6 × 10^{-3} mol/g·s (a factor of ~2× greater for the co-precipitated catalysts). These kinetic changes result in very similar steady-state TOF values of 1.4 and 1.5 × 10^{-3}/s at 265 °C for the 1VTi(I) and 1VTi(C) catalysts, respectively. This suggests that the presence of the new surface VO_x sites and surface defects introduced by vanadia co-impregnation on the TiO_2 support does not have a significant effect on the SCR reaction kinetics.

The addition of surface WO_x to the impregnated 1VTi(I) catalyst to give the 1V5WTi(I) catalyst slightly increases the Ea, within experimental error, and increases the pre-exponential factor by ~3×. In addition, the surface WO_x sites also increase the catalyst surface area from 40 to 54 m^2/g (factor of ~1.35×). These changes correspond to only a small increase in the SCR TOF from 1.4 to 1.7 × 10^{-3}/s (~1.2×) at 265 °C for the impregnated 1VTi(I) to 1V5WTi(I) catalysts, respectively.

The addition of WO_x to the synthesis of the co-precipitated 1V5WTi(C) catalyst has a more pronounced effect on the SCR performance. Although Ea increases slightly (from 49 to 54 kJ/mol), the pre-exponential factor increases by almost an order of magnitude. This leads to increasing the SCR TOF for the co-precipitated catalysts at 265 °C from 1.5 × 10^{-3}/s for 1VTi(C) to 4.8 × 10^{-3}/s 1V5WTi(C), a factor ~3.2×. The SCR TOF for the co-precipitated 1V5WTi(C) catalyst is also ~3× greater than the corresponding impregnated 1V5WTi(I) catalyst. It appears that WO_x is the component most responsible for creating a poorly ordered and defective TiO_2(anatase) support that is responsible for enhancing the ammonia adsorption capacity of the co-precipitated 1V5WTi(C) catalyst.

Many publications suggest that high SCR activity is related to high number of surface Brønsted acid sites, but the current study finds that for two catalysts with the same composition and BET surface area that the catalyst with the lower number of surface Brønsted acid sites, 1V5WTi(C), is more active than the catalyst with a higher number of surface Brønsted acid sites, 1V5WTi(I). The enhanced activity of the co-precipitated 1V5WTi(C) catalyst is most likely related to the presence of greater number of titania surface defects present for this catalyst.

It has been proposed in the SCR literature that strong electronic interactions between surface tungsta and vanadia species and the titania support cause synergism between the surface vanadia and tungsta sites that promotes the redox activity of V_2O_5-WO_3/TiO_2 catalysts for the SCR reaction relative to the analogous V_2O_5-TiO_2 catalysts [7,64–66]. The current NO/NH_3/O_2 SCR kinetics do not demonstrate a marked synergistic activity between the 1VTi(I) and 1V5WTi(I) catalysts. If synergistic electronic interactions between surface VO_x-WO_x sites were present, they would also be expected to affect the redox activity of other oxidation reactions (*e.g.*, CH_3OH oxidation to HCHO [67] and SO_2 oxidation to SO_3 [68]), but promotion of surface VO_x by surface WO_x is not observed for these other oxidation reactions. The modest enhancement in the SCR kinetics introduced by impregnation of surface WO_x sites to the VTi(I) catalyst is related to a catalyst with higher surface area and, thus, increased adsorption capacity for ammonia [7,56]. In spite of the claim in the SCR catalysis literature about the promoting effect of WO_x on VO_x sites on TiO_2, there is no supporting evidence for an electronic interaction between surface VO_x and WO_x sites on TiO_2 supports [56].

The comparison between 1VTi(I) and 1V5WTi(I) also allows addressing another claim in the SCR catalysis literature that oligomeric surface VO_4 sites on TiO_2 are more active than isolated surface VO_4 sites on TiO_2 [69,70]. The 1VTi(I) catalyst exhibits the symmetric stretch of the surface O = VO_4 site at 1027 cm^{-1} while the corresponding vibration appears at 1037 cm^{-1} for the 1V5WTi(I) catalyst indicating a higher degree of oligomerization of the surface VO_4 sites on the 1V5WTi(I) catalyst. The TOF values at 265 °C for the 1VTi(I) and 1V5WTi(I) catalysts are 1.4× and 1.7 × 10^{-3}/s. Even if the mild promotion by the surface WO_5 sites is ignored, this only yields an increase of ~20% (factor of ~1.2×), which is not significantly different and demonstrates that extent of oligomerization of surface VO_4 sites on TiO_2 does not have a significant effect on the SCR TOF value.

5. Conclusions

This is the first investigation to compare side-by-side impregnated and co-precipitated VWTi SCR catalysts to determine the differences and similarities between these two preparation methods. Co-precipitated and impregnated WTi, VTi and VWTi catalysts contain oligomerized surface mono-oxo O = VO_3 and O = WO_4 sites on the TiO_2 support. The co-precipitated W- and V-containing catalysts also possess new surface O = WO_4 and O = VO_3 sites, respectively, ascribed to anchoring at surface defects of the TiO_2 support. Both surface NH_4^{+*} and NH_3^* intermediates are present on all the catalysts and addition of surface O = WO_4 species to V-containing catalysts increases the ratio of surface NH_4^{+*}/NH_3^* intermediates. No relationship, however, could be found between the SCR activity and the population of surface NH_4^{+*} and NH_3^* intermediates. The $NO/NH_3/O_2$ SCR reaction is dominated by the redox surface mono-oxo O = VO_3 sites and the role of the surface O = WO_4 sites is to enhance adsorption of ammonia, which is greater for the co-precipitated catalysts. Consequently, the SCR activity is always greater for the co-precipitated catalysts for the same catalyst composition and surface area. The enhanced performance of co-precipitated compared to the impregnated VWTi catalysts is associated with the larger capacity for ammonia adsorption, which is thought to be related to the greater amount of surface defects on the TiO_2(C) support relative to the low amount of defects on the highly crystallineTiO_2(P-25) support. There is no electronic promotion of the surface VO_4 sites by the surface WO_5 sites as hypothesized in the literature since the SCR rates are almost the same for 1VTi(I) and 1V5WTi(I) catalysts.

Acknowledgments

Ms. Yuanyuan He is grateful for financial support from the China Scholarship Council (CSC) for the State Scholarship and National Natural Science Funds of China (Nos. 51274263 and 51204220). Prof. I.E. Wachs, Drs. Tumuluri and Wu were supported by the Center for Understanding & Control of Acid Gas-Induced Evolution of Materials for Energy (UNCAGE-ME), an Energy Frontier Research Center funded by DOE, Office of Science, Office of Basic Energy Sciences under grant DE-SC0012577). A portion of this research including the isotopic exchange was conducted at the Center for Nanophase Materials Sciences, which is a DOE office of the Science User Facility. The authors thank Y. Tang, D. G. Gregory, C. J. Keturakis, and Ms. Q. Guo of Lehigh University for experimental assistance.

Appendix A. Supplementary data

Supplementary data associated with this article can be found, in the online version, at http://dx.doi.org/10.1016/j.apcatb.2016.04.022.

References

[1] L. Lietti, J. Svachula, P. Forzatti, G. Busca, G. Ramis, F. Bregani, Catal. Today 17 (1993) 131–139.
[2] G. Busca, L. Lietti, G. Ramis, F. Berti, Appl. Catal. B 18 (1998) 1–36.
[3] P. Forzatti, Appl. Catal. A 222 (2001) 221–236.
[4] S.C. Wood, Chem. Eng. Prog. 90 (1994) 32–38.
[5] P. Forzatti, L. Lietti, Heterog. Chem. Rev. 3 (1996) 33–51.
[6] P. Forzatti, I. Nova, E. Tronconi, A. Kustov, J.R. Thogersen, Catal. Today 184 (2012) 153–159.
[7] L.J. Alemany, L. Lietti, N. Ferlazzo, P. Forzatti, G. Busca, E. Giamello, F. Bregani, J. Catal. 155 (1995) 117–130.
[8] M. Kobayashi, K. Miyoshi, Appl. Catal. B 72 (2007) 253–261.
[9] S.M. Lee, S.S. Kim, S.C. Hong, Chem. Eng. Sci. 79 (2012) 177–185.
[10] M.D. Amiridis, R.V. Duevel, I.E. Wachs, Appl. Catal. B 20 (1999) 111–122.
[11] M.D. Amiridis, I.E. Wachs, G. Deo, J.M. Jehng, D.S. Kim, J. Catal. 161 (1996) 247–253.
[12] G.C. Bond, Appl. Catal. A 157 (1997) 91–103.
[13] S. Djerad, L. Tifouti, M. Crocoll, W. Weisweiler, J. Mol. Catal. A: Chem. 208 (2004) 257–265.
[14] G. Cristallo, E. Roncari, A. Rinaldo, F. Trifiro, Appl. Catal. A 209 (2001) 249–256.
[15] G. Madia, M. Elsener, M. Koebel, F. Raimondi, A. Wokaun, Appl. Catal. B 39 (2002) 181–190.
[16] I. Nova, L.D. Acqua, L. Lietti, E. Giamello, P. Forzatti, Appl. Catal. B 35 (2001) 31–42.
[17] N.Y. Topsoe, H. Topsoe, J.A. Dumesic, J. Catal. 151 (1995) 226–240.
[18] N.Y. Topsoe, J.A. Dumesic, H. Topsoe, J. Catal. 151 (1995) 241–252.
[19] I.E. Wachs, R.Y. Saleh, S.S. Chan, C. Chersich, Chem. Technol. 15 (1985) 756–761.
[20] L.J. Alemany, F. Berti, G. Busca, G. Ramis, D. Robba, G.P. Toledo, M. Trombetta, Appl. Catal. B 10 (1996) 299–311.
[21] J.P. Chen, R.T. Yang, J. Catal. 139 (1993) 277–288.
[22] I.E. Wachs, J.M. Jehng, G. Deo, B.M. Weckhuysen, V.V. Guliants, J.B. Benziger, S. Sundaresan, J. Catal. 170 (1997) 75–88.
[23] M. Waqif, J. Bachelier, O. Saur, J.C. Lavalley, J. Mol. Catal. 72 (1992) 127–138.
[24] M.A. Vuurman, I.E. Wachs, A.M. Hirt, J. Phys. Chem. 95 (1991) 9928–9937.
[25] I.E. Wachs, C.A. Roberts, Chem. Soc. Rev. 39 (2010) 5002–5017.
[26] A. Khodakov, B. Olthof, A.T. Bell, E. Iglesia, J. Catal. 181 (1999) 205–216.
[27] G.T. Went, S.T. Oyama, A.T. Bell, J. Phys. Chem. 94 (1990) 4240–4246.
[28] P.G.W.A. Kompio, A. Bruckner, F. Hipler, G. Auer, E. Loffler, W. Grunert, J. Catal. 286 (2012) 237–247.
[29] M.A. Reiche, P. Hug, A. Baiker, J. Catal. 192 (2000) 400–411.
[30] M.A. Reiche, T. Burgi, A. Baiker, A. Scholz, B. Schnyder, A. Wokaun, Appl. Catal. A 198 (2000) 155–169.
[31] M.A. Reiche, E. Ortelli, A. Baiker, Appl. Catal. B 23 (1999) 187–203.
[32] H. Zhang, J. Han, X.W. Niu, X. Han, G.D. Wei, W. Han, J. Mol. Catal. A: Chem. 350 (2011) 35–39.
[33] K.K. Akurati, A. Vital, J.P. Dellemann, K. Michalow, T. Graule, D. Fetti, A. Baiker, Appl. Catal. B 79 (2008) 53–62.
[34] T. Onfroy, V. Lebarbier, G. Clet, M. Houalla, J. Mol. Catal. A: Chem. 318 (2010) 1–7.
[35] A. Scholz, B. Schnyder, A. Wokaun, J. Mol. Catal. A: Chem. 138 (1999) 249–261.
[36] W.Q. Liu, X.H. Liu, J.Y. Zhang, J. Petrochem. Univ. 1 (2003) 1–4.
[37] V. Lebarbier, G. Clet, M. Houalla, J. Phys. Chem. B 110 (2006) 22608–22617.
[38] P. Patrono, A. Laginestra, G. Ramis, G. Busca, Appl. Catal. A 107 (1994) 249–266.
[39] F.C. Jentoft, H. Schmelz, H. Knozinger, Appl. Catal. A 161 (1997) 167–182.
[40] C.A. Carrero, C.J. Keturakis, A. Orrego, R. Schomacker, I.E. Wachs, Dalton Trans. 42 (2013) 12644–12653.
[41] J. Rouquerol, D. Avnir, C.W. Fairbridge, D.H. Everett, J.H. Haynes, N. Pernicone, J.D.F. Ramsay, K.S.W. Sing, K.K. Unger, Pure Appl. Chem. 66 (1994) 1739–1758.
[42] G. Deo, A.M. Turek, I.E. Wachs, T. Machej, J. Haber, N. Das, H. Eckert, A.M. Hirt, Appl. Catal. A 91 (1992) 27–42.
[43] E.I. Ross-Medgaarden, I.E. Wachs, W.V. Knowles, A. Burrows, C.J. Kiely, M.S. Wong, J. Am. Chem. Soc. 131 (2009) 680–687.
[44] I.R. Beattie, T.R. Gilson, Proc. R. Soc. Lond. Ser. A 307 (1968) 407.
[45] I.R. Beattie, T.R. Gilson, J. Chem. Soc. A (1969) 2322–2327.
[46] N. Magg, B. Immaraporn, J.B. Giorgi, T. Schroeder, M. Baumer, J. Dobler, Z.L. Wu, E. Kondratenko, M. Cherian, M. Baerns, P.C. Stair, J. Sauer, H.J. Freund, J. Catal. 226 (2004) 88–100.
[47] T. Kim, I.E. Wachs, J. Catal. 255 (2008) 197–205.
[48] E.I. Ross-Medgaarden, I.E. Wachs, J. Phys. Chem. C 111 (2007) 15089–15099.
[49] I.E. Wachs, T. Kim, E.I. Ross, Catal. Today 116 (2006) 162–168.
[50] Z.L. Wu, A.J. Rondinone, I.N. Ivanov, S.H. Overbury, J. Phys. Chem. C 115 (2011) 25368–25378.
[51] G. Busca, J. Raman Spectrosc. 33 (2002) 348–358.
[52] Y. Li, Z.H. Wei, F. Gao, L. Kovarik, C.H.F. Peden, Y. Wang, J. Catal. 315 (2014) 15–24.
[53] L. Lietti, J.L. Alemany, P. Forzatti, G. Busca, G. Ramis, E. Giamello, F. Bregani, Catal. Today 29 (1996) 143–148.
[54] J.M.G. Amores, V.S. Escribano, G. Ramis, G. Busca, Appl. Catal. B 13 (1997) 45–58.
[55] L. Lietti, I. Nova, S. Camurri, E. Tronconi, P. Forzatti, AlChE J. 43 (1997) 2559–2570.

[56] G. Ramis, G. Busca, C. Cristiani, L. Lietti, P. Forzatti, F. Bregani, Langmuir 8 (1992) 1744–1749.
[57] J. Datka, A.M. Turek, J.M. Jehng, I.E. Wachs, J. Catal. 135 (1992) 186–199.
[58] M.D. Amiridis, J.P. Solar, Ind. Eng. Chem. Res. 35 (1996) 978–981.
[59] J. Marangozis, Ind. Eng. Chem. Res. 31 (1992) 987–994.
[60] L. White, G. Duffy, Ind. Eng. Chem. 51 (1959) 232–238.
[61] M. Baron, H. Abbott, O. Bondarchuk, D. Stacchiola, A. Uhl, S. Shaikhutdinov, H.J. Freund, C. Popa, M.V. Ganduglia-Pirovano, J. Sauer, Angew. Chem. Int. Ed. 48 (2009) 8006–8009.
[62] T. Kim, A. Burrows, C.J. Kiely, I.E. Wachs, J. Catal. 246 (2007) 370–381.
[63] C.B. Wang, Y.P. Cai, I.E. Wachs, Langmuir 15 (1999) 1223–1235.
[64] L. Lietti, P. Forzatti, F. Bregani, Ind. Eng. Chem. Res. 35 (1996) 3884–3892.
[65] M.C. Paganini, L. DallAcqua, E. Giamello, L. Lietti, P. Forzatti, G. Busca, J. Catal. 166 (1997) 195–205.
[66] L. Lietti, Appl. Catal. B 10 (1996) 281–297.
[67] I.E. Wachs, Catal. Today 100 (2005) 79–94.
[68] J.P. Dunn, H.G. Stenger, I.E. Wachs, J. Catal. 181 (1999) 233–243.
[69] G.T. Went, L.J. Leu, R.R. Rosin, A.T. Bell, J. Catal. 134 (1992) 492–505.
[70] A. Baiker, B. Handy, J. Nickl, M. Schramlmarth, A. Wokaun, Catal. Lett. 14 (1992) 89–99.